High-dimensional mass cytometry reveals emphysema-associated changes in the pulmonary immune system

Jia, L.; Li, N.; Abdelaal, T.R.M.; Guo, N.N.; Ijsselsteijn, M.E.; Unen, V. van; ... ; Khedoe, P.P.S.J.

ORIGINAL ARTICLE

High-Dimensional Mass Cytometry Reveals Emphysema-associated Changes in the Pulmonary Immune System

Li Jia[1,4*], Na Li[1,5*], Tamim R. M. Abdelaal[2,6,7], Nannan Guo[1], Marieke E. IJsselsteijn[3], Vincent van Unen[1], Ciska Lindelauf[1], Qinyue Jiang[1], Yanling Xiao[1], M. Fernanda Pascutti[1], Pieter S. Hiemstra[4], Frits Koning[1], Jan Stolk[4], and P. Padmini S. J. Khedoe[4]

[1]Department of Immunology, [2]Department of Radiology, [3]Department of Pathology, and [4]Department of Pulmonology, PulmoScience Lab, Leiden University Medical Center, Leiden, the Netherlands; [5]State Key Laboratory for Diagnosis and Treatment of Severe Zoonotic Infectious Diseases, Key Laboratory of Zoonosis Research of the Ministry of Education, Institute of Zoonosis and College of Veterinary Medicine, Jilin University, Changchun, China; [6]Systems and Biomedical Engineering Department, Faculty of Engineering, Cairo University, Giza, Egypt; and [7]Pattern Recognition and Bioinformatics, Delft University of Technology, Delft, the Netherlands

ORCID ID: 0000-0002-0798-014X (P.P.S.J.K.).

Abstract

Rationale: Chronic inflammation plays an important role in alveolar tissue damage in emphysema, but the underlying immune alterations and cellular interactions are incompletely understood.

Objectives: To explore disease-specific pulmonary immune cell alterations and cellular interactions in emphysema.

Methods: We used single-cell mass cytometry (CyTOF) to compare the immune compartment in alveolar tissue from 15 patients with severe emphysema and 5 control subjects. Imaging mass cytometry (IMC) was applied to identify altered cell–cell interactions in alveolar tissue from patients with emphysema ($n = 12$) compared with control subjects ($n = 8$).

Measurements and Main Results: We observed higher percentages of central memory CD4 T cells in combination with lower proportions of effector memory CD4 T cells in emphysema. In addition, proportions of cytotoxic central memory CD8 T cells and $CD127^+CD27^+CD69^-$ T cells were higher in emphysema, the latter potentially reflecting an influx of circulating lymphocytes into the lungs. Central memory CD8 T cells, isolated from alveolar tissue from patients with emphysema, exhibited an IFN-γ response upon anti-CD3 and anti-CD28 activation. Proportions of $CD1c^+$ dendritic cells, expressing migratory and costimulatory markers, were higher in emphysema. Importantly, IMC enabled us to visualize increased spatial colocalization of $CD1c^+$ dendritic cells and CD8 T cells in emphysema *in situ*.

Conclusions: Using CyTOF, we characterized the alterations of the immune cell signature in alveolar tissue from patients with chronic obstructive pulmonary disease stage III or IV emphysema versus control lung tissue. These data contribute to a better understanding of the pathogenesis of emphysema and highlight the feasibility of interrogating the immune cell signature using CyTOF and IMC in human lung tissue.

Clinical trial registered with www.clinicaltrials.gov (NCT04918706).

Keywords: severe emphysema; pulmonary immune compartment; central memory T cells; single-cell mass cytometry; imaging mass cytometry

(Received in original form March 13, 2023; accepted in final form March 27, 2024)

*Co–first authors.

Supported by Chinese Scholarship Council grant 201906170073 (L.J.), TAS-ZonMW grant 40414009816007 (J.S.), and Leiden University Fund grant W223064-2-32 (P.P.S.J.K.).

Author Contributions: L.J., N.L., C.L., Q.J., and P.P.S.J.K. performed the experiments, processed the data, and prepared the manuscript. T.R.M.A. performed data normalization/analyses. N.G., M.E.IJ., V.v.U., Y.X., and M.F.P. provided intellectual input for the manuscript. P.P.S.J.K., J.S., F.K., and P.S.H. designed and supervised the project and contributed to writing the manuscript. All authors have read the manuscript and approve its submission.

Correspondence and requests for reprints should be addressed to P. Padmini S. J. Khedoe, Ph.D., Department of Pulmonology, PulmoScience Lab, Leiden University Medical Center, Albinusdreef 2, 2333 ZA Leiden, the Netherlands. E-mail: p.p.s.j.khedoe@lumc.nl.

This article has a related editorial.

A data supplement for this article is available via the Supplements tab at the top of the online article.

Am J Respir Crit Care Med Vol 210, Iss 8, pp 1002–1016, Oct 15, 2024

Originally Published in Press as DOI: 10.1164/rccm.202303-0442OC on March 27, 2024
Internet address: www.atsjournals.org

At a Glance Commentary

Scientific Knowledge on the Subject: Very recently published manuscripts show that IFN-γ–producing lymphocytes suppress the regeneration of alveolar stem cells, and higher numbers of IFN-γ–producing CD8 T lymphocytes in pre- and terminal bronchioles of patients with chronic obstructive pulmonary disease (COPD) suppress terminal airway–enriched secretory cells, thereby driving emphysema. Specific CD8 subsets and their secretome thereby may provide novel therapeutic targets for treatment of COPD patients with emphysema.

What This Study Adds to the Field: Using the state-of-the art techniques single-cell mass cytometry and imaging mass cytometry, we characterized the immune cells in alveolar tissue from emphysema and control lungs and identified emphysema-specific alterations in myelocytes and lymphocytes. CD8 T-cell subsets derived from alveolar emphysema tissue showed an augmented IFN-γ response upon T cell receptor–engaged activation. In our study, we furthermore showed increased colocalization of CD8 T cells and $CD1c^+$ dendritic cells in emphysema using spatial visualization, likely reflecting interactions between these cells in emphysema. Thereby, these data contribute to a better understanding of the altered immune cell profiles and cellular spatial colocalization in emphysema and highlight the feasibility of interrogating the immune cell signature using single-cell and imaging mass cytometry in human lung tissue.

Chronic obstructive pulmonary disease (COPD) is the third-largest cause of mortality worldwide (1). In the majority of patients with COPD, progressive inflammation causes irreversible alveolar tissue damage (emphysema) leading to impaired gas exchange and loss of lung function (2), which severely impacts the quality of life of patients with emphysema. Both cigarette smoking and exacerbations (sudden worsening in the clinical course of the disease caused by, e.g., infections) result in inflammatory responses that play an important role in emphysema pathogenesis. Furthermore, inflammation often persists in those who have successfully quit smoking (3).

Various immune cell subsets have been implicated in chronic inflammation and emphysema in COPD. Effector cytotoxic T cells expressing Granzyme B (Gr-B) may contribute to loss of alveolar tissue (4–6). Activated lung-resident dendritic cells (DCs) (7), but also circulating DCs (8), release proinflammatory cytokines, which lead to T helper cell recruitment and activation in COPD. Furthermore, increased numbers of lung macrophages have been found to produce higher amounts of chemokines and cytokines (9), whereas some studies also suggest a dysfunction of lung macrophages (10, 11). Although several immune subsets have been shown to drive disease pathogenesis in the airways of patients with COPD (12, 13), a system-wide approach to interrogate the immune subsets and immune cellular interactions in the affected alveolar lung tissue in emphysema is still lacking. To better understand the mechanisms that lead to emphysema development, it is crucial to characterize the COPD emphysematous microenvironment with a multidimensional approach, which allows the simultaneous interrogation of immune cell subsets across multiple lineages and delineation of the immune cells and structural cells *in situ*. Single-cell mass cytometry (CyTOF) allows a high-dimensional approach (14) to characterize the immune cell composition in detail (15, 16) using up to 40 markers simultaneously, which enables unraveling of the immune cell complexity and heterogeneity based on phenotypic hierarchical cell clustering (17–19). Tissue architecture and cellular complexity can be analyzed with imaging mass cytometry (IMC) (20), in which the tissue complexity and heterogeneity can be explored by visualizing the cellular composition, distribution, localization, and cellular interactions in the tissue context (21).

In our study, we examined the immune cell composition, localization, and cellular interactions in alveolar tissue from patients with emphysema versus control distal lung tissue using CyTOF and IMC. Using this approach, we aimed to identify disease-associated changes in the composition of the immune compartment in severe emphysema compared with control subjects.

Some of the results of these studies have been previously reported in the form of an abstract (22).

Methods

Human Samples Used in the Current Study

Alveolar tissue was obtained from patients with severe emphysema ($n = 15$; Global Initiative for Chronic Obstructive Lung Disease stage III or IV) undergoing lung volume reduction surgery as part of a clinical trial (NCT04918706); all patients provided informed consent. Control alveolar lung tissue ($n = 5$ patients) was collected from macroscopically normal lung tissue obtained from patients undergoing resection surgery for lung cancer at the Leiden University Medical Center, the Netherlands. These patients were enrolled in a biobank via a no-objection system for coded anonymous further use of such tissue (www.federa.org). However, since January 9, 2022, patients are enrolled in the biobank using active informed consent in accordance with local regulations from the Leiden University Medical Center biobank, with approval by the institutional medical ethical committee (B20.042/Ab/ab and B20.042/Kb/kb). For the present study, only tissue collected before January 9, 2022 was used, and, therefore, individual informed consent was not required. Clinical characteristics are summarized in Table 1. Details regarding inclusion and exclusion criteria for included patients are provided in the supplemental methods (*see* online supplement).

Freshly collected lung tissue from resection or lung volume reduction surgery was processed according to an adapted version of a previously published protocol (16). A detailed description of tissue processing can be found in the supplemental methods.

The use of alveolar tissue from patients with emphysema for research purpose was approved by the Central Committee on Research Involving Human Subjects of the Netherlands, and all study participants gave written consent. The study was registered at ClinicalTrials.gov: http://clinicaltrials.gov/study/NCT04918706.

Table 1. Clinical Characteristics

Study	Group, *P* Value	Age	Sex (F/M)	FEV_1 (% Predicted)	D_{LCO} (% Predicted)	FEV_1/FVC	Pack-Years	Emphysema Score (or HU)
CyTOF	Control ($n=5$)	67.60 ± 5.6	4/1	96.4 ± 6.3	78.40 ± 6.9	71.75 ± 4.2	25.2 ± 9.6	−908 ± 8.0
	Emphysema ($n=15$)	57.00 ± 2.7	10/5	31.93 ± 1.8	35.79 ± 3.1	33.24 ± 1.6	24.1 ± 8.4	−965.5 ± 4.5
	P value	0.0006	—	0.0001	0.0003	0.042	NS	0.0002
Functional spectral flow cytometry*	Control ($n=3$)	68.67 ± 3.9	2/1	101.0 ± 9.2	85.00 ± 8.0	77.00 ± 4.9	—	−899 ± 4.3
	Emphysema ($n=3$)	57.00 ± 1.2	2/1	32.67 ± 3.8	30.00 ± 2.0	31.00 ± 3.0	—	−966 ± 9.8
	P value	NS	—	NS	NS	NS	—	NS
Snap-frozen IMC*	Control ($n=3$)	70.67 ± 2.0	2/1	70 ± 8.9	79.67 ± 17.0	70.00 ± 1.	—	−898.7 ± 9.60
	Emphysema $n=9$)	57.89 ± 1.7	6/3	34.01 ± 2.4	38.00 ± 4.5	34.01 ± 1.5	—	−964.4 ± 5.4
	P value	0.0091	—	0.0444	0.0182	0.0444	—	0.0091
FFPE IMC†	Control ($n=8$)	66.00 ± 2.0	5/3	99.13 ± 5.8	89.13 ± 5.6	74.63 ± 2.6	—	Unknown
	Emphysema ($n=12$)	57.00 ± 1.6	8/4	31.92 ± 2.4	35.73 ± 3.4	33.34 ± 1.7	—	−965.5 ± 4.4
	P value	0.0014	—	<0.0001	<0.0001	<0.0001	—	—

Definition of abbreviations: CyTOF = single-cell mass cytometry; FFPE = formalin-fixed paraffin-embedded; HU = Hounsfield units; IMC = imaging mass cytometry; NS = not significant.
All values represent means per group ± SEM. All participants were ex-smokers and all participants were White. All included patients with chronic obstructive pulmonary disease with emphysema (Global Initiative for Chronic Obstructive Lung Disease stage III or IV) used long-acting bronchodilators and inhaled corticosteroids, whereas the control subjects with lung cancer did not use these medications.
*The samples that were used for spectral flow cytometry and snap-frozen IMC experiments are part of samples included in the CyTOF study.
†For FFPE IMC measurements, we included additional historically collected control ($n=3$) and emphysema ($n=1$) samples.

CyTOF

Procedures for mass cytometry antibody staining and data acquisition were performed as described before (18). Data analysis was performed as described previously (23). Detailed information on staining procedure and data analysis are available in Tables E1 and E2 in the online supplement and the supplemental methods.

Functional Analyses of T Cells Using Spectral Flow Cytometry

Unfractionated single lung cells from the alveolar tissue of patients with emphysema ($n=3$) and control subjects ($n=3$) were collected to extend the CyTOF data and determine cytokine production upon anti-CD3 and anti-CD28 T-cell receptor (TCR)-engaged stimulation using spectral flow cytometry. Procedures for spectral flow cytometry are performed as described before (24). Detailed information on cell stimulation, staining procedure, and data analysis are available in the supplemental methods and Table E3.

IMC in Snap-Frozen and Formalin-fixed Paraffin-embedded Lung Tissue

Procedures for IMC antibody staining and data acquisition for snap-frozen tissue were performed as previously described (21, 23, 25): for snap-frozen lungs, we used a 36-antibody IMC panel of immune and lung structural markers (antibodies are listed in Table E4) and analyzed sections of snap-frozen human alveolar tissue samples from patients with emphysema ($n=8$) and control ($n=3$) lung tissue. For formalin-fixed paraffin-embedded (FFPE) lung tissue, a 34-antibody IMC panel was used to analyze FFPE sections of human alveolar tissue samples from patients with emphysema ($n=12$) and control ($n=8$) lung tissue (Table E5). Detailed information on the staining procedure is included in the supplemental methods. For IMC analyses, alveolar tissue areas from both groups were randomly selected microscopically. In alveolar tissue from patients with emphysema, areas with severe alveolar destruction as well as adjacent areas, where alveolar septa were still present, were analyzed. However, for comparison between the groups, we focused on tissue areas where alveolar septa were still present to enable identification of immune cell infiltrates. Areas with severe emphysema (Figure E7A, right image), large vessels, and large and small airways were excluded from IMC analyses. All IMC data were analyzed by Fluidigm MCD viewer (v1.0.560.2) as described in (15). Sixteen-bit TIFF files of each region of interest (ROI) were exported from MCD viewer and imported in Cytosplore Imaging to perform an interactive visual analysis. Data were sample-tagged and transformed in Cytosplore Imaging using Arcsinh transformation with cofactor 5, resampling option 2, and Bi-cubic interpolation (15). Cell clusters were identified after Hierarchical Stochastic Neighbor Embedding (HSNE) analysis and were quantified by pixel analysis. IMC data were also confirmed by cell segmentation using Illastik, as described before (26, 27). Additional details of experimental procedures for CyTOF and IMC measurements and analyses are provided in the supplemental information.

Statistical Analysis

All results are reported as means ± SEM. All data were analyzed using unpaired nonparametric Mann-Whitney *U* test for comparisons between groups in GraphPad version 9.3.1. *P* values < 0.05 were considered statistically significant. For IMC data, average values of multiple ROIs per donor were compared using unpaired nonparametric Mann-Whitney *U* test for comparisons between groups. As the age differed significantly between the groups for various experiments, all data were analyzed and corrected for age using linear regression analysis between the dependent variable age, and all measured outcome parameters were appropriate.

Results

Proportions of Major Immune Lineages Are Comparable between Alveolar Tissue from Patients with Emphysema and Control Lung Tissue

The lymphoid antibody panel (Table E1) was used to analyze CyTOF suspensions from 5 control lung samples and 15 emphysema

lung samples (Figure 1A). HSNE analysis was performed in Cytosplore on all acquired $CD45^+$ cells (Figures 1B and E1A) to determine the immune composition. Based on the expression of major immune lineage markers, we identified $CD3^+CD4^+$ T cells, $CD3^+CD8^+$ T cells, $CD11c^+$ myeloid cells, $CD19^+$ B cells, $CD3^-CD7^+$ natural killer (NK) cells, and innate lymphoid cells (ILCs) (Figures 1B and 1C). Although we observed a large heterogeneity in proportions of major immune lineages within $CD45^+$ cells among samples, there was no difference between control samples and alveolar tissue from patients with emphysema (Figures 1D and 1E). Following a similar approach with the myeloid antibody panel (Table E2), we identified myeloid populations (Figures E1B and E1C) with substantial heterogeneity between samples (Figure E1D), although myeloid and NK cell proportions were comparable between control and emphysema lungs (Figure E1E).

Proportions of $CD161^+CD69^-$ CD4 Central Memory T Cells, $CD127^+CD27^+CD69^-$ CD4 Central Memory T Cells, and Effector Memory T Cells Are Enriched in Alveolar Tissue from Patients with Emphysema

To explore the composition of the lymphocyte compartment in control and alveolar tissue from patients with emphysema in more detail, we analyzed the major immune lineages separately at the single-cell level. CD4 T cells (8.13×10^5 cells) were clustered based on the marker expression profiles identifying five main CD4 T-cell populations (Figures 2A–2C and E2A), namely naive CD4 T cells (CD4 Tn, $CCR7^+CD45RO^-$), central memory CD4 T cells (CD4 Tcm, $CCR7^+CD45RO^+$), effector memory CD4 T cells (CD4 Tem, $CCR7^-CD45RO^+$), terminally differentiated CD4 T cells (CD4 Temra, $CCR7^-CD45RA^+$), and regulatory T cells (Treg, $Foxp3^+$). Although the proportion of the Tn, Temra, and Treg populations did not differ between control subjects and patients with emphysema (Figure E2B), alveolar tissue from patients with emphysema exhibited significantly higher proportions of CD4 Tcm (emphysema: 22.17 ± 1.36; control: 16.37 ± 1.78; P value = 0.04) and significantly lower proportions of CD4 Tem (emphysema: 62.17 ± 1.73; control: 72.71 ± 3.92; P value = 0.02) (Figure 2D), which was confirmed by manual gating using FlowJo (Figure E4A) and spectral flow cytometry analysis (Figure E4D). We therefore zoomed in on all CD4 Tcm cells using t-distributed stochastic neighbor embedding analysis at the single-cell level and clustered these into seven subpopulations based on the marker expression profiles (Figures 2E and E2C). Within the CD4 Tcm population, proportions of T-helper cell type 17 (Th17)-associated $CD127^+CD27^+CD161^+CD69^-$ cells (clusters 6 and 7) (28), distinguished by chemokine receptor C-X-C motif chemokine receptor 3 (CXCR3) expression, were significantly higher in alveolar tissue from patients with emphysema (3.092 ± 0.41) compared with control subjects (0.9825 ± 0.22; P value = 0.002; Figure 2F). These CD4 Tcm cells were able to produce IL-17A upon anti-CD3 and anti-CD28 activation (Figure E2G). Moreover, percentages of $CD127^+CD27^+CXCR3^{+/-}$ cells were significantly higher in alveolar tissue from patients with emphysema compared with control subjects (emphysema: 9.280 ± 3.34; control 4.892 ± 0.93; P value = 0.019; Figure 2F; clusters 8–11). Proportions of the non–tissue-resident $CD127^+CD27^+CD69^-$ CD4 Tcm cells were also significantly higher in alveolar tissue from patients with emphysema compared with control tissue (emphysema: 13.31 ± 1.15; control: 6.365 ± 1.30; P value = 0.0037; Figures 2F and E2D).

We next focused on the CD4 Tem population, in which we distinguished five subpopulations (Figure 2G). Within this population, percentages of the tissue-resident $CD69^+$ CD4 Tem population (clusters 1–5) were significantly lower in alveolar tissue from patients with emphysema compared with control subjects (emphysema: 34.30 ± 3.75; control: 56.39 ± 7.02; P value = 0.0328; Figure 2H). In contrast, the percentage of non–tissue-resident $CD127^+CD27^+CD69^-$ CD4 Tem cells (clusters 8 and 9) was higher in emphysema than control tissue (emphysema: 15.04 ± 1.63; control: 7.940 ± 0.45; P value = 0.0054; Figures 2H and E2F). These non–tissue-resident $CD161^+$ CD4 Tem were able to produce IL17A upon anti-CD3 and anti-CD28 activation (Figure E2G).

Altogether, within the CD4 T-cell compartment, we observed higher proportions of CD4 Tcm cells combined with lower CD4 Tem cells in emphysema. Especially, percentages of CD4 Tcm and CD4 Tem cells, characterized by a Th17-associated $CD161^+$ phenotype, which had the capacity to produce IL17A upon TCR-engaged activation (Figure E2G), were higher in the alveolar tissue of patients with emphysema than in control samples. Moreover, we identified abundant non–tissue-resident $CD127^+CD27^+CD69^-$ CD4 Tcm and Tem cells in severe emphysema, whereas the percentage of tissue-resident $CD69^+$ CD4 Tem cells was lower. These data reflect a potential influx of circulating CD4 memory T cells into alveolar tissue of patients with emphysema.

CD8 Tcm and Tem Subsets Have a Cytotoxic Phenotype in Emphysema and Display an IFN-γ Response upon TCR-engaged Activation

We next analyzed the CD8 and γδ T cells (8.10×10^5 cells) in more detail. First, using HSNE analysis, the CD8 and γδ T cells were grouped into five main populations, namely naive CD8 T cells (CD8 Tn, $CCR7^+CD45RO^-$), central memory CD8 T cells (CD8 Tcm, $CCR7^+CD45RO^+$), effector memory CD8 T cells (CD8 Tem, $CCR7^-CD45RO^+$), terminally differentiated CD8 T cells (CD8 Temra, $CCR7^-CD45RA^+$), and γδ T cells (γδ T, TCR $\gamma\delta^+$) (Figures 3A–3C). The proportion of CD8 Tn, CD8 Tem, CD8 Temra, and γδ T cells was comparable between the groups (Figures E3A and E3B), although the CD8 Temra population was very heterogeneous among samples. Percentages of CD8 Tcm cells were higher in alveolar tissue from patients with emphysema (emphysema: 15.89 ± 1.59; control: 8.658 ± 2.39; P value = 0.0328; Figure 3D), which we also confirmed by manual gating using FlowJo (Figure E4B) and spectral flow cytometry (Figure E4E). CD8 Tcm cells were divided in eight subpopulations (Figure 3E). We observed significantly higher percentages of $CD27^+CD127^+CXCR3^+$ CD8 Tcm cells (clusters 15 and 16) in emphysema, which also expressed the transcription factor T-bet (emphysema: 1.531 ± 0.31; control: 0.3724 ± 0.18; P value = 0.0037; Figure 3F). A small subpopulation, which was almost exclusively present in alveolar tissue from patients with emphysema (cluster 19), expressed the proliferation marker Ki-67 and transcription factor GATA-3 (emphysema: 0.08106 ± 0.03; control: 0.00887 ± 0.004; P value = 0.0252; Figure 3F). In line with our findings in the CD4 T-cell compartment, proportions of non–tissue-resident $CD127^+CD27^+CD69^-$ CD8 Tcm cells

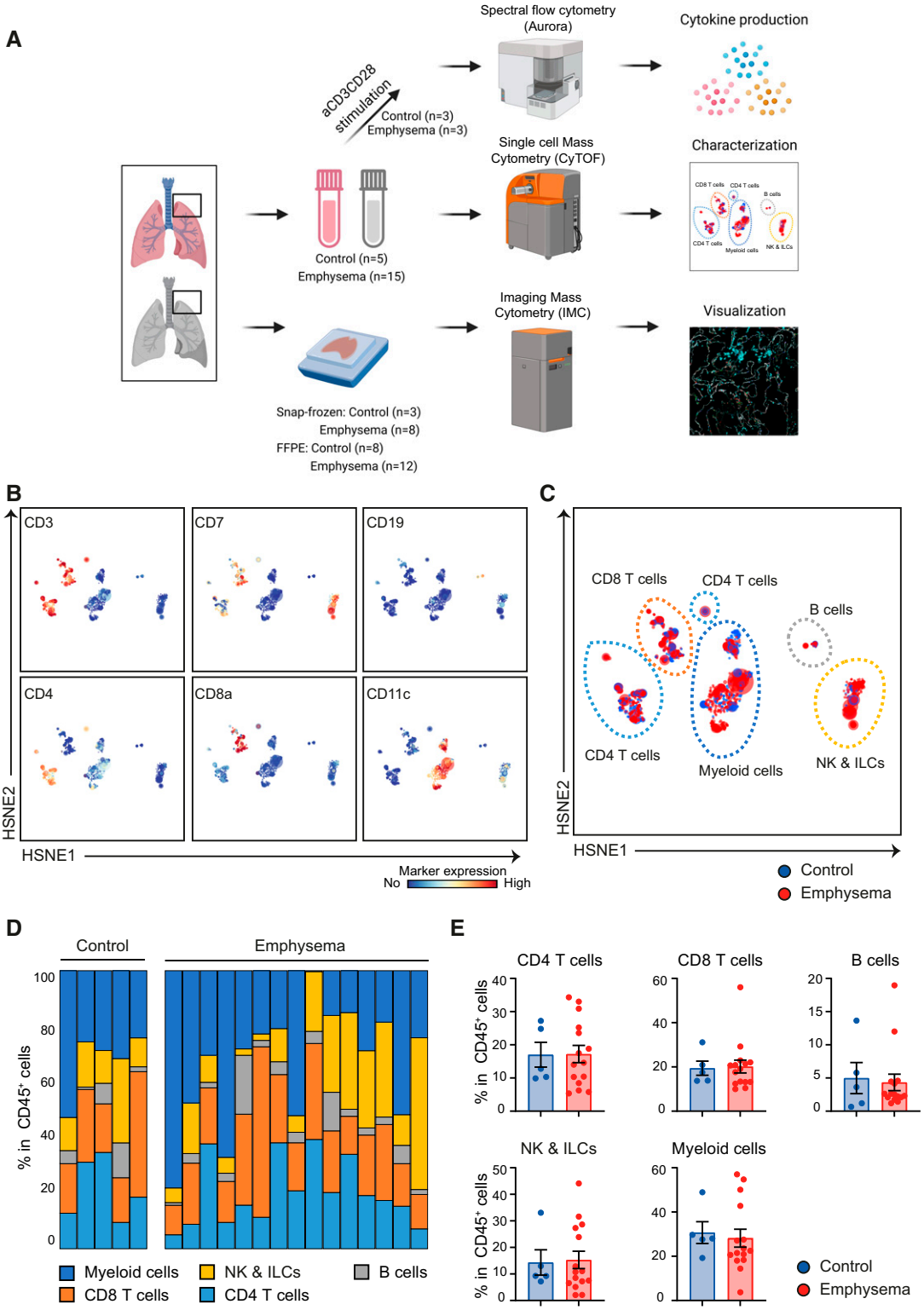

Figure 1. Hierarchical Stochastic Neighbor Embedding (HSNE) analysis identifies major immune lineages across alveolar tissue from patients with emphysema and control lung tissue. (*A*) Freshly collected control lung tissue from resection ($n = 5$) or emphysematous lung volume resection surgery ($n = 15$) was processed for single-cell isolation after Ficoll-gradient separation. Cells were stored until analysis for single-cell mass cytometry (CyTOF) and functional spectral flow cytometry studies. Single-cell suspension was measured by CyTOF, and major immune lineages were visualized by high-dimensional analysis. Lung cells isolated from alveolar tissue from patients with emphysema or control lungs ($n = 3$ per group) were stimulated by anti-CD3 and anti-CD28 to determine cytokine production using spectral flow cytometry. For imaging mass

(clusters 8–10 and 13–19) were significantly higher in patients with emphysema (emphysema: 5.776 ± 0.81; control: 2.793 ± 0.82; *P* value = 0.0254; Figures 3F and E3D).

Although CD8 Tem cells were not significantly different between control subjects and patients, we did explore the CD8 Tem population by hierarchical clustering (Figure E3E). Proportions of cytotoxic Gr-B$^+$T-bet$^+$Eomes$^+$ CD8 Tem subpopulations (clusters 6–9) and non–tissue-resident CD27$^+$CD127$^+$CD69$^-$ CD8 Tem subpopulations (clusters 21 and 22) expressing CXCR3 and T-bet or GATA-3 were higher in alveolar tissue from patients with emphysema (Figure E3F).

Because we observed an enrichment of CD8 Tcm in alveolar tissue from patients with emphysema, we next evaluated the functionality of the CD8 Tcm compartment in the lungs. We applied spectral flow cytometry to assess cytokine production in unfractionated single cells derived from alveolar tissue from patients with emphysema or control subjects upon TCR-engaged activation by anti-CD3 and anti-CD28 stimulation. Activated CD8 Tcm cells derived from both control samples and alveolar tissue from patients with emphysema showed elevated IFN-γ production and CD40L expression compared with nonstimulated samples (Figure 3G). Furthermore, although nonsignificant because of the low sample size per group, we observed elevated IFN-γ production with higher mean fluorescence intensities within the activated CD8 Tcm from emphysema samples compared with control samples (Figure 3H), suggesting an upregulation of the IFN-γ response in emphysema. Similarly, elevated amounts of IFN-γ producing CD4 Tcm subsets from alveolar tissue from patients with emphysema were observed upon TCR-engaged activation (Figure E4F). Other T-cell–related cytokines were measured as well in CD4 and CD8 Tcm and Tem subsets upon anti-CD3 and anti-CD28 activation, including IL-2, IL-17A, IL-22, and tumor necrosis factor-α (Figures E4F–E4I).

Collectively, we observed abundant non–tissue-resident CD127$^+$CD27$^+$CD69$^-$ CD8 Tcm and CD8 Tem cells, and higher cytotoxic Gr-B$^+$T-bet$^+$ CD8 Tcm and CD8 Tem cells in alveolar tissue from patients with severe emphysema. Furthermore, CD8 Tcm cells isolated from alveolar tissue of patients with emphysema showed an augmented IFN-γ response upon TCR-engaged activation.

NK Cells, ILCs, and B Cells Are Unaltered in Emphysema

Analyses of the CD3$^-$CD7$^+$ cells, including NK cells and ILCs, did not reveal differences between the control and emphysema samples (Figures E5A–E5D), with the exception of cluster 3 (CD161$^+$CD127$^+$CD38$^+$GATA-3$^+$T-bet$^+$Eomes$^+$) within ILCs, which was enriched in patients with emphysema (Figure E5D). Furthermore, although we observed a large heterogeneity in B-cell proportions, we did not reveal differences between the control and emphysema samples (Figures E5E–E5G). We confirmed B-cell heterogeneity in hematoxylin and eosin–stained images, elucidating the presence of lymphoid follicle-like structure exclusively in some emphysema samples (Figure E5H).

Activated CD1c$^+$ DCs Are Enriched in Alveolar Tissue from Patients with Emphysema

Next, we selected the CD3$^-$CD19$^-$ HLA-DR$^+$ myeloid cell population (1.1×10^6 cells), which we identified using the myeloid antibody panel (Figures 4A and E1C). We performed HSNE analysis and identified five phenotypically distinct subpopulations: macrophages (MΦ, CD68$^+$/CD163$^+$), classical monocytes (CD14$^+$), intermediate and nonclassical monocytes (CD11c$^+$CD206$^-$CD14$^{+/-}$ CD16$^{+/-}$), plasmacytoid DCs (pDCs, CD123$^+$CD11c$^-$), and DCs (CD1c$^+$) (Figures 4A–4C). Although there were no differences in proportions of macrophages, monocytes, and pDCs (Figure E6A), the percentage of CD1c$^+$ DCs was significantly higher in alveolar tissue from patients with emphysema compared with control lungs (emphysema: 20.09 ± 3.01; control: 6.960 ± 1.79; *P* value = 0.0077; Figure 4D). We subsequently zoomed in on each myeloid cell population, which did not reveal significant differences in macrophages, monocytes, and pDC subpopulations among the groups (Figures E6B–E6F). However, detailed analysis of the CD1c$^+$ DCs characterized two phenotypical DC subpopulations (Figure 4E), including cDC2 (CD11c$^+$CD1c$^+$CD14$^-$) and monocyte-derived DC (moDC) (CD1c$^+$CD11b$^+$CD14$^+$CD206^{hi}). Some cDC2s had a mature regulatory DC (mreg-like DC) phenotype (CD1c$^+$CD40$^+$CD80$^+$PD-L1$^+$PD-L2$^+$). Percentages of cDC2 (emphysema: 13.59 ± 2.95; control: 5.019 ± 1.37; *P* value = 0.0146) and moDC (emphysema: 6.072 ± 1.10; control: 1.615 ± 0.39; *P* value = 0.0021) were higher in emphysema and expressed the costimulatory markers CD86 and CCR2 (Figure 4F). Collectively, in alveolar tissue from patients with emphysema, we detected a higher proportion of migratory cDC2 and moDC that expressed CCR2, characterized by a CD40$^{+/-}$ CD86$^+$ activated phenotype.

Spatial Analysis Reveals Heterogeneity in the Macrophages and Frequent Interaction of CD1c$^+$ DCs and CD8 T Cells in Alveolar Tissue from Patients with Severe Emphysema

To validate the results obtained with CyTOF and gain insight into the spatial distribution

Figure 1. (*Continued*). cytometry (IMC), lung tissue sections were processed in Tissuetag (snap-frozen) or formalin fixed and thereafter paraffin embedded (FFPE) and stored until analysis. Snap-frozen and FFPE lung tissue sections were measured by IMC, after which the immune cell composition, localization, and cellular interactions were explored *in situ*. (*B* and *C*) A collective HSNE analysis was performed on all acquired CD45$^+$ immune cells (4.3×10^6 cells) derived from lung tissue across control subjects ($n = 5$) and patients with emphysema ($n = 15$) at the overview level. Each dot represents an HSNE landmark, and the size of the landmark indicates the number of cells. The color scale indicates the degree of marker expression (blue: no or low expression; red: high expression). (*D*) The composition of the major immune populations within total CD45$^+$ immune cells in control and emphysema lung samples is represented by vertical bars; the length of the colored segment represents the proportion of cells as percentage of CD45$^+$ cells in the sample. Colors represent different populations within the CD45$^+$ immune cells. (*E*) The frequencies of major immune lineage populations were calculated as percentage of total CD45$^+$ immune cells among the control and emphysema groups. Bars indicate means ± SEM; each dot represents an individual sample. ILC = innate lymphoid cell; NK = natural killer.

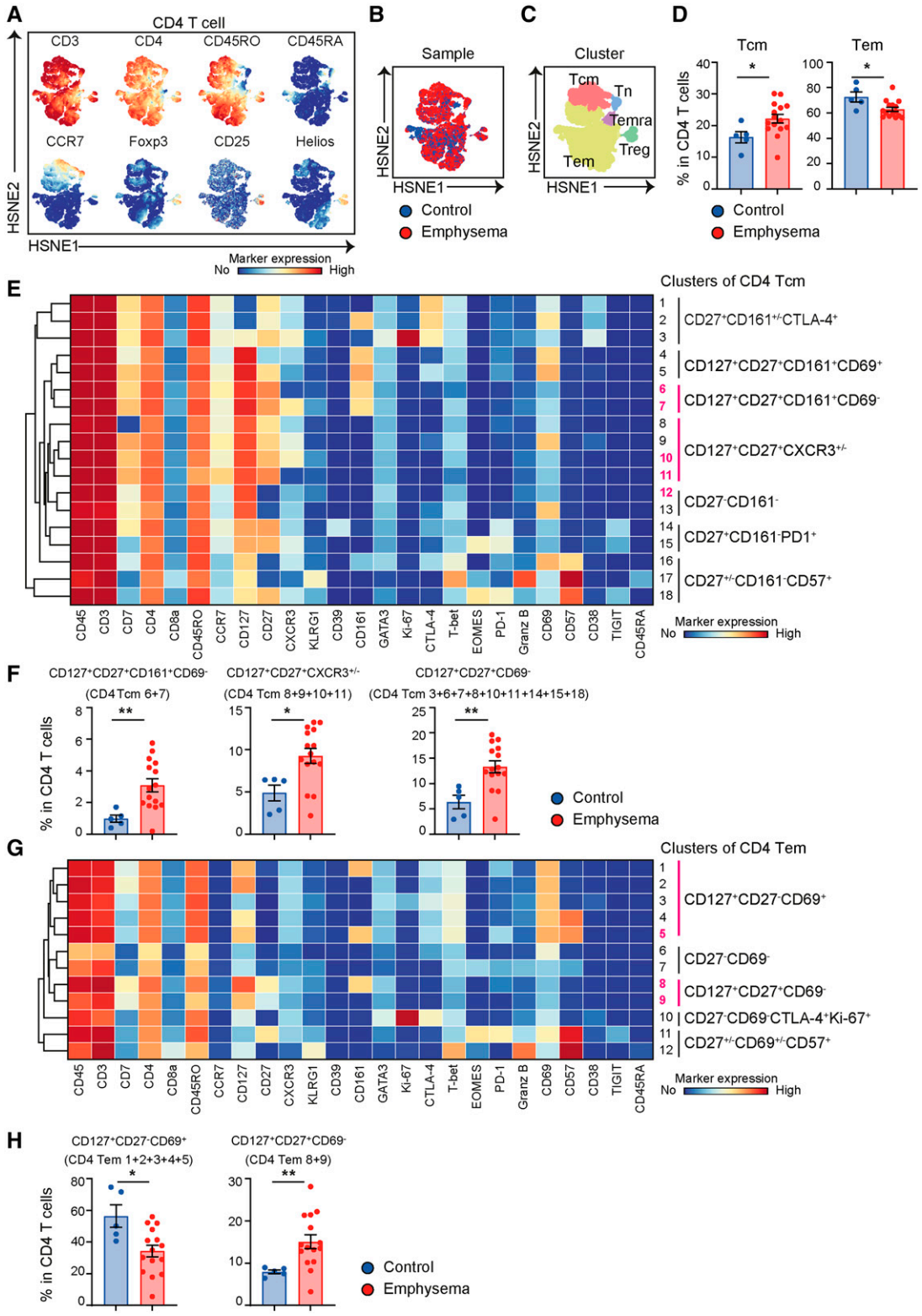

Figure 2. Identification of phenotypically distinct clusters in the CD4 T-cell compartment across the control and emphysema groups. (*A–C*) A collective Hierarchical Stochastic Neighbor Embedding (HSNE) analysis was performed on CD4 T cells (total, 8.13×10^5 cells) derived from lung tissue across control subjects ($n = 5$) and patients with emphysema ($n = 15$). Naive (Tn), central memory (Tcm), effector memory (Tem), terminally differentiated (Temra), and regulatory (Treg) T cell populations were visualized in an HSNE plot. (*D*) From the HSNE analysis, frequencies of Tcm and Tem cell populations were calculated among control subjects and patients with emphysema as percentage of total

of the immune compartment in emphysema, we performed IMC on snap-frozen and FFPE alveolar lung tissue sections from control subjects and patients with emphysema (Figures 1A and E7A); areas with severe alveolar tissue loss were excluded from IMC analyses. The 36- and 34-antibody IMC panels visualized the lung tissue architecture, including HTI-56 or Surfactant Protein-C (alveolar type 1 or type 2 cells, AEC1 and AEC2 cells, respectively), CD31 (endothelial cells), collagen I (extracellular matrix), and distinguished various immune cell subsets (Tables E4 and E5). Based on the expression of immune lineage markers, we visualized $CD3^-CD7^+$ cells, $CD3^+CD4^+$ T cells, $CD3^+CD8a^+$ T cells, $CD1c^+$ DCs, and $CD66b^+$ neutrophils, which were located in the alveolar wall (Figures 5A, E7B, and E7C).

Next, with Cytosplore Imaging, we quantified cell-type–specific pixels to determine the density of the major immune cell lineages in snap-frozen and FFPE lung tissue sections. In agreement with the single-cell data, higher numbers of $CD1c^+$ DCs were revealed in patients with emphysema compared with control subjects (emphysema: 6.593 ± 0.79; control: 3.728 ± 0.36; P value = 0.0182; Figure 5B), which were confirmed in validated FFPE lung samples using pixel and cell segmentation analysis (emphysema: 0.4782 ± 0.05; control: 0.2816 ± 0.03; P value = 0.0055; Figure 5C). Other immune lineages were comparable among groups (Figures E7F and E7G). Similarly, we detected heterogeneity in the macrophage compartment as well (Figures 5D and E8A–E8D), which were located in both luminal space and interstitial lung tissue. $CD206^+CD68^{+/-}CD163^+$ macrophages (pink arrows) were located in the alveolar wall. Two major $CD206^+CD68^+$ macrophage subsets, distinguished by the absence or presence of CD163 (orange and green arrows), were present in the air space (Figures 5D and E8). Pixel quantification (emphysema: 14.93 ± 2.48; control: 5.403 ± 0.89; P value = 0.0182; Figure 5E) and cell segmentation analysis (emphysema: 0.1125 ± 0.02; control: 0.04389 ± 0.005; P value = 0.0073; Figure 5F) revealed higher numbers of $CD206^+CD163^-$ macrophages in the air space of alveolar tissue from patients with emphysema compared with control alveolar tissue.

We then focused on cellular interactions within the lung tissue and observed frequent colocalization of $CD1c^+$ DCs with CD8 T cells in alveolar tissue from patients with severe emphysema (Figures 6A and 6B). Quantification of the frequency of these interactions by pixel analysis indicated more common interactions in emphysema compared with control lungs (emphysema: 0.4322 ± 0.09; control: 0.4322 ± 0.08; P value = 0.0091; Figures 6C and 6D), which we confirmed by manual counting and neighborhood analyses (Figure E9).

Collectively, using IMC, we were able to comprehensively visualize all major immune subsets *in situ* and detected substantial heterogeneity within the lung macrophages in agreement with the CyTOF data. Furthermore, we showed more frequent colocalization between $CD1c^+$ DCs and CD8 T cells in lungs of patients with emphysema, suggestive of involvement of these interactions in disease pathogenesis.

Discussion

In this study, we observed higher percentages of central memory CD4 T cells and cytotoxic central memory CD8 T cells in alveolar tissue from patients with emphysema. We also show higher proportions of $CD127^+CD27^+CD69^-$ T cells potentially reflecting an influx of circulating lymphocytes into the lungs. Upon isolation from alveolar tissue from patients with emphysema, central memory CD8 T cells were found to exhibit a higher IFN-γ response after anti-CD3 and anti-CD28 activation. Furthermore, the percentage of $CD1c^+$ dendritic cells expressing migratory and costimulatory markers was higher in emphysema. Importantly, using IMC, we visualized increased spatial colocalization of $CD1c^+$ dendritic cells and CD8 T cells in emphysema *in situ*.

The relative abundant $CD69^-$ T lymphocyte populations, observed in alveolar tissue from patients with emphysema, possibly reflecting recruitment of peripheral cells, displayed a $CD127^+CD27^+$ phenotype, which may contribute to inflammatory responses in the lung (29). Moreover, we observed higher proportions of CD4 Tcm in emphysema, in line with a previous study that studied patients with disease of similar severity (30). However, in contrast to previous studies (31, 32), we observed lower CD4 Tem in patients with emphysema. Importantly, we observed that $CD161^+$ CD4 T cells, which are able to produce IL-17A upon anti-CD3 and anti-CD28 activation, were more abundant in alveolar tissue from patients with emphysema, suggesting a local role for a Th17 phenotype (33). This phenotype has been reported to be increased in peripheral blood of patients with COPD (28), but so far not in lung tissue. These results are in line with previous findings implying a Th17 and Treg imbalance contributing to COPD development (34).

Within the CD8 T-cell compartment, we observed various differences between control and emphysema lungs. The most significant difference was observed in $CD27^+CD127^+CXCR3^+$ CD8 Tcm, suggestive of an inflammatory phenotype (35). These cells potentially contribute to parenchymal lung damage (36) through release of MMP-9 (matrix metalloproteinase-9), CXCR3-mediated Tn activation, and lymphocyte migration (37). Although present at low percentages, the $GATA\text{-}3^+Ki\text{-}67^+$ proliferating subset of CD8 Tcm cells was almost exclusively present in alveolar tissue from patients with emphysema. Importantly, this subset has been described to secrete a variety of proinflammatory and cytotoxic mediators (38), which likely contribute to alveolar tissue damage and decreased lung function.

Figure 2. (*Continued*). CD4 T cells. (*E*) The mean marker expression values were visualized in a heatmap, from which CD4 Tcm cell clusters were identified (blue: no or low expression; red: high expression). Numbers or lines in pink indicate clusters or subpopulations that differ significantly between control subjects and patients with emphysema. (*F*) The frequencies of the identified CD4 Tcm cell populations were calculated as percentage of CD4 T cells among the control and emphysema groups. (*G*) Expression of the mean marker values are visualized in a heatmap, through which CD4 Tem cell clusters were identified (blue: no or low expression; red: high expression). (*H*) The frequencies of the identified CD4 Tem cell clusters are calculated as percentage of total CD4 T cells in both groups. Bars indicate means ± SEM; each dot represents an individual sample. $^*P < 0.05$ and $^{**}P < 0.01$ by Mann-Whitney U test. Tcm = $CCR7^+CD45RO^+$ CD4 T cell; Tem = $CCR7^-CD45RO^+$ CD4 T cell; Temra = $CCR7^-CD45RA^+$ CD4 T cell; Tn = $CCR7^+CD45RO^-$ CD4 T cell; Treg = $Foxp3^+$ regulatory T cell.

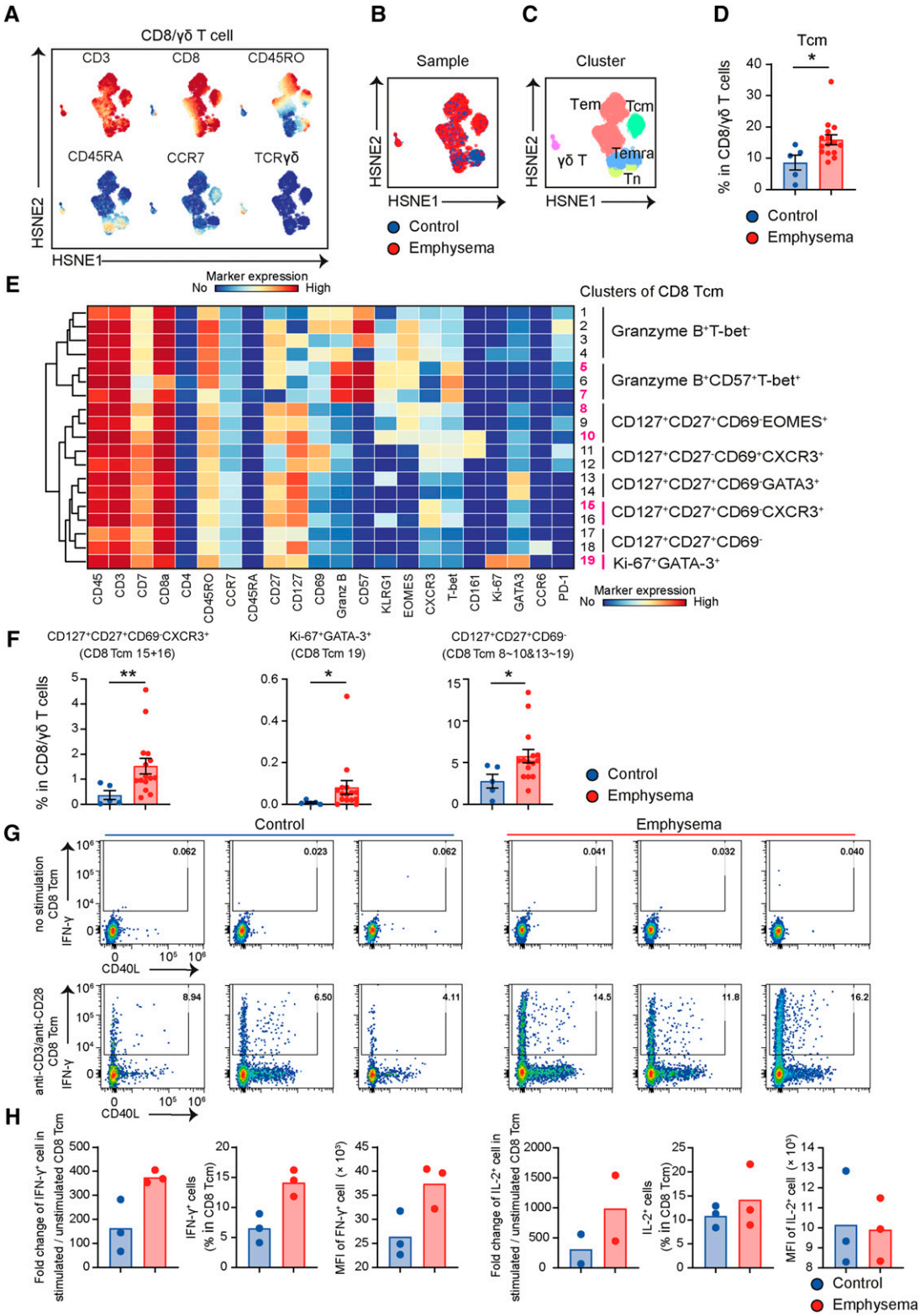

Figure 3. Identification of phenotypically and functionally distinct clusters within the CD8 T-cell compartment between control and emphysema lungs. (*A–C*) A collective Hierarchical Stochastic Neighbor Embedding (HSNE) analysis was performed on $CD8^+$ and γδ T cells (total, 8.10×10^5 cells) derived from lung tissue from control subjects ($n = 5$) and patients with emphysema ($n = 15$). Naive (Tn), central memory (Tcm), effector memory (Tem), terminally differentiated (Temra), and γδ T cell populations were visualized in an HSNE plot. (*D*) From the HSNE analysis, frequencies of Tcm cell population were calculated among control subjects and patients with emphysema as percentage of total

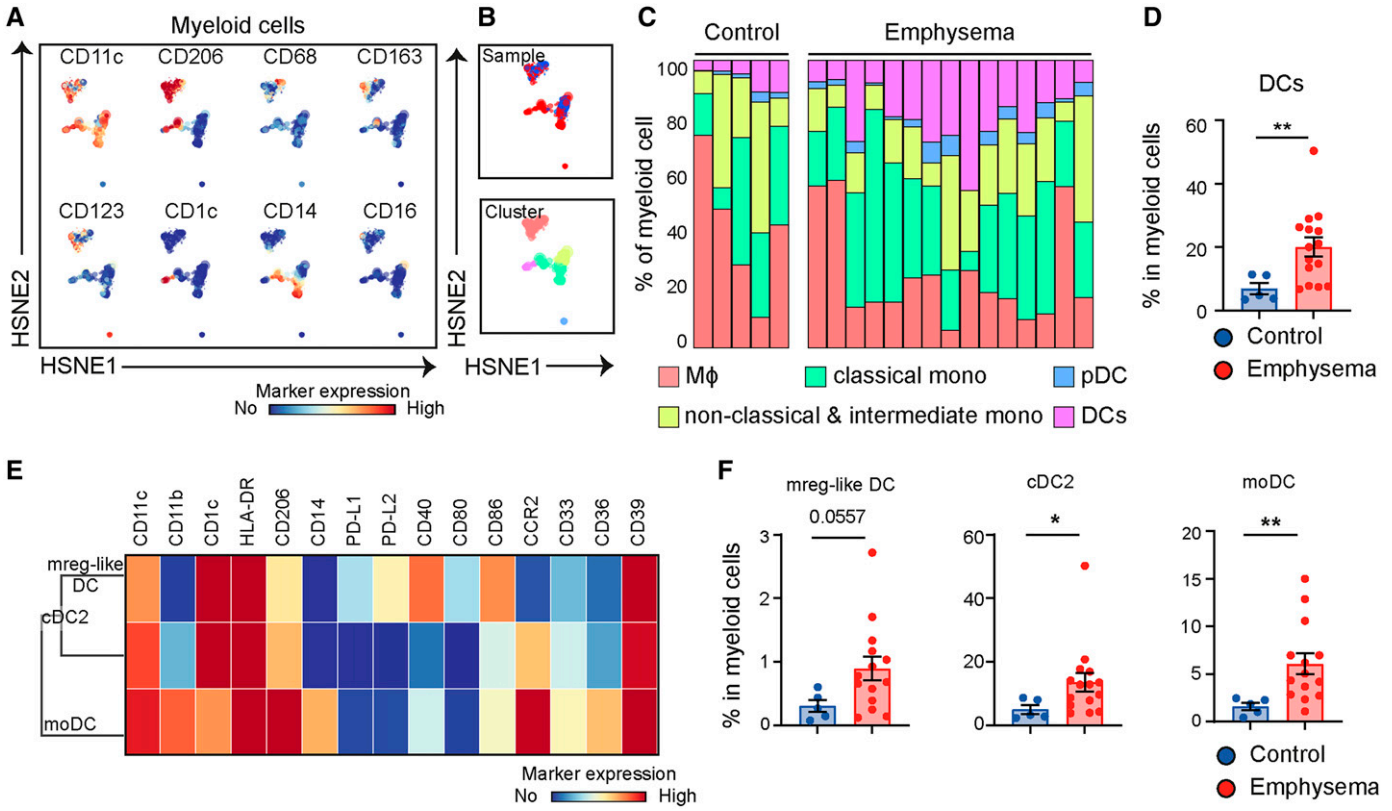

Figure 4. Identification of phenotypically distinct clusters in the myeloid compartment across the control and emphysema groups. (*A* and *B*) A collective Hierarchical Stochastic Neighbor Embedding (HSNE) analysis was performed on myeloid cells (1.1×10^6 cells) derived from lung tissue across control subjects ($n = 5$) and patients with emphysema ($n = 15$). MΦ ($CD68^+/CD163^+$), classical monocyte ($CD14^+$), nonclassical and intermediate monocyte ($CD14^{+/-}CD16^{+/-}$), dendritic cell (DC, $CD1c^+$), and plasmacytoid DC ($CD123^+$) populations were visualized in an HSNE plot. (*C*) The composition of the five myeloid populations in control and emphysema lung samples is represented by vertical bars, where the length of the colored segment represent the proportion of cells as percentage of myeloid cells. Colors represent different populations within myeloid cells. (*D*) The frequency of the $CD1c^+$ DC population was calculated as percentage of the total myeloid cells in control subjects and patients with emphysema. (*E*) Mean marker expression values were visualized in a heatmap, from which 2 $CD1c^+$ cell clusters were identified (blue: no or low expression; red: high expression). (*F*) The frequencies of the identified DC subpopulations were calculated as percentage of total myeloid cells among the control and emphysema group. Bars indicate means ± SEM; each dot represents an individual sample. $^*P < 0.05$ and $^{**}P < 0.01$ by Mann-Whitney *U* test. MΦ = macrophage.

Finally, a CD8 Tcm subset that was higher in alveolar tissue from patients with emphysema was characterized by the cytotoxic markers Gr-B, Eomes, and T-bet. Previously, Gr-B^+ CD8 Tcm cells were suggested to contribute to emphysema progression (39). This T-bet^+ population potentially indicates an exhausted phenotype mediating impaired immune responses (40), thereby contributing to alveolar damage. Importantly, compared with control lungs, in emphysema we found a higher frequency of CD8 T cells, especially CD8 Tcm, which were able to produce IFN-γ upon anti-CD3 and anti-CD28 activation. These observations are in line with recent findings showing that lymphocyte-derived IFN-γ suppresses the regeneration of alveolar stem cells (41) and terminal airway–enriched secretory cells (42), thereby preventing tissue repair in

Figure 3. (*Continued*). CD8 T cells. (*E*) Mean marker expression values were visualized in a heatmap, from which CD8 Tcm cell clusters were identified (blue: no or low expression; red: high expression). Numbers or lines in pink indicate clusters or subpopulations that differ significantly between control subjects and patients with emphysema. (*F*) The frequencies of the indicated CD8 Tcm cell populations were calculated as percentage of total CD8 T cells among the control and emphysema groups. Bars indicate mean ± 95% confidence interval; each dot represents an individual sample. (*G*) Single cells derived from control lung tissue and alveolar tissue from patients with emphysema were stimulated with vehicle or anti-CD3 and anti-CD28 for 6 hours, after which intracellular expression of IFN-γ was determined in the CD8 Tcm population by spectral flow cytometry. (*H*) The fold change of IFN-γ^+ cells in stimulated compared with unstimulated CD8 Tcm cells. The proportion and the MFI of IFN-γ^+ cells were calculated. Similar analyses were performed for IL-2^+ cells. Samples in blue and red represent control and emphysema samples, respectively. Bars indicate means or means ± SEM; each dot indicates an individual sample. $^*P < 0.05$ and $^{**}P < 0.05$ by Mann-Whitney *U* test. γδ T = γδ$^+$ T cell; MFI = mean fluorescence intensity; Tcm = $CCR7^+CD45RO^+$CD8 T cell; Tem = $CCR7^-CD45RO^+$CD8 T cell; Temra = $CCR7^-CD45RA^+$CD8 T cell; Tn = $CCR7^+CD45RO^-$CD8 T cell.

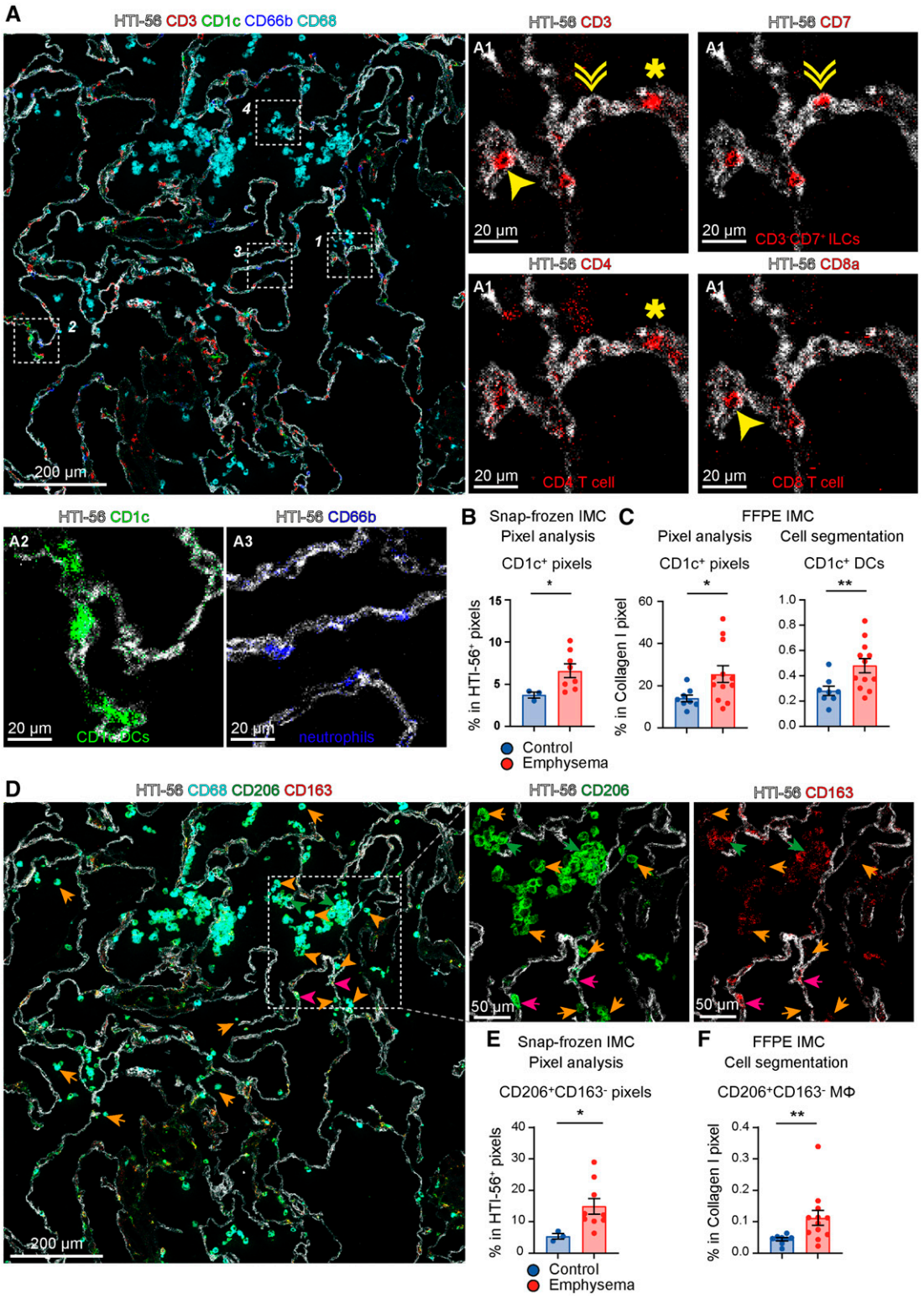

Figure 5. Spatial imaging analyses reveal heterogeneity in the immune cell composition in alveolar tissue from patients with emphysema. (*A*) Imaging mass cytometry (IMC) was performed and several (immune, structural) markers were visualized, including: $CD3^{-}CD7^{+}$ natural killer and innate lymphoid cells (double arrow), CD4 T cells (stars), CD8a T cells (yellow arrows), $CD1c^{+}$ dendritic cells (DCs, green), $CD66b^{+}$ neutrophils (blue), and $CD68^{+}$ macrophages (light blue). $CD1c^{+}$ DC in (*B*) snap-frozen or (*C*) formalin-fixed paraffin-embedded (FFPE) tissue. IMC images were analyzed using pixel quantification or cell segmentation. (*D*) Different macrophage subsets were visualized: $CD206^{+}CD68^{+}CD163^{-}$ macrophages (orange arrows), $CD206^{+}CD68^{+}CD163^{+}$ macrophages (green arrows) and $CD206^{+}CD68^{+}CD163^{+}$

emphysema (43). Furthermore, another study showed that subsets of cytotoxic CD8 T cells interact with myeloid cells and alveolar cells, which was also mediated by IFN-γ (44). In our study, we observed that IFN-γ–producing cells from alveolar tissue from patients with emphysema were also able to produce IL-2 upon TCR-engaged activation. Future functional studies exploring the impact of these altered cytokine profiles within CD4 and CD8 T-cell subsets on lung tissue repair and regeneration are warranted to investigate potential therapeutic implications for patients with COPD with emphysema.

In the B-cell compartment, we observed a large heterogeneity between samples in the CyTOF analysis, which could be explained by the presence of lymphoid-like follicular structures in eight emphysema samples, whereas these were less abundant in the control samples. Previous studies showed increased numbers of B cells and inducible bronchus associated lymphoid tissue structures in especially severe emphysema (45–49). Histological assessment of such structures in our study revealed the presence of such structures mainly nearby airway structures, which we largely excluded from our IMC analyses, and is in line with previous findings (50, 51). Although we mainly selected subpleural distal alveolar lung tissue for the CyTOF study, we cannot exclude the presence of some airway structures in the single-cell suspensions, which may have contributed to the heterogeneity in B-cell proportions and subsets.

We also observed significantly higher numbers of $CD1c^+$ DCs in patients with emphysema, in line with other studies (30, 52, 53). Our study adds to these findings by demonstrating a significantly higher number of $CD1c^+$ DCs expressing the costimulatory CD40 and CD86 in emphysema, suggesting an increased capacity for T-cell activation (54). In addition, the IMC analysis revealed a significant increase in colocalization of $CD1c^+$ DCs and CD8 T cells in emphysema that may be involved in disease pathogenesis. Indeed, murine studies have shown that DCs and CD8 T cells contribute to emphysema development through CD40 and CD40L interactions, and drive Th1 cell differentiation (55).

Although we observed a large heterogeneity in macrophage subsets (9) in distal lung tissue between samples using CyTOF analysis, we found no significant differences in major macrophage subsets, which is in line with human single-cell RNA sequencing data (56). Other studies did report alterations in the phenotype (11) or numbers (57) of alveolar macrophages in COPD. This difference may partly result from the use of defrosted lung cells in our study, which may have caused the loss of some macrophages. Furthermore, within the myeloid compartment, we observed more $CD206^+CD68^+CD163^-$ alveolar macrophages in emphysema using IMC, a subset that may contribute to proinflammatory responses (58).

Despite providing a detailed analysis and localization of various immune subsets in alveolar tissue from patients with emphysema, our study has some limitations.

First, we used tumor-free resected lung tissue as controls because we have no access to healthy lung tissue. Both the control patients, who had normal spirometry and gas transfer, and patients with emphysema, are ex-smokers, which may explain the finding that there were no differences in the major immune lineages between the groups.

Second, we observed a large heterogeneity in the proportions of various immune cell lineages in both alveolar tissue from patients with emphysema and control lung tissue, which can partly be explained by variations in the anatomical location of the tissue (upper or lower lobes, left or right lung) and presence of fibrotic tissue in the emphysema group. As the ventilation/perfusion ratios may differ significantly between moderate to severe emphysema and lungs with normal spirometry and gas transfer, differences in blood perfusion between emphysema and control lungs may also have contributed in part to the presence and heterogeneity in various immune cells. Also, although lung tissue was extensively washed to remove excess blood, access to blood vessels for application of vascular perfusion was technically impossible before processing. Therefore, we cannot exclude the presence of cells from the vasculature in the obtained samples.

Third, in this study, because of technical limitations, we could not inflate the obtained pieces of lung tissue and, therefore, were unable to follow principles of stereology and microscopically assess alveolar tissue loss or mean linear intercept between the groups. The included ROIs, therefore, may potentially be subject to technical artifacts during sample processing, which we addressed by including historically stored FFPE tissue samples and increasing the sample size per group for imaging analyses. Future studies applying standardized methods of sampling, tissue inflation, and selection of areas of interest with mildly and severely affected areas of emphysema are necessary to provide detailed insight into the altered cellular interactions in these areas. In our IMC studies, we excluded areas with severe emphysema (low number or absence of alveolar septa), because of the low cell numbers present in these areas, which complicated proper analyses and interpretation of data. Furthermore, in the single-cell analyses (CyTOF and spectral flow cytometry), we used digested tissue, which may have been heterogeneous in composition, consisting of conducting and respiratory airways (remodeling, small airway disease), arterioles, and venous vasculature changes, and may have influenced some of our findings.

Fourth, overall, the number of subjects included in this study was quite small. This small sample size may explain part of the lack of significant differences between the control and emphysema groups presented in Figures 1D and 1E. Although we were able to confirm the higher proportions of CD8 T cells and $CD1c^+$ DCs and colocalization of these cells in emphysema lungs in historically stored FFPE lung tissue blocks, future studies using larger sample size numbers are necessary for a better understanding of the location, priming, and interaction of such immune cells in the pathogenesis of COPD. Despite these limitations, using high-dimensional CyTOF and IMC technology, we did find

Figure 5. (*Continued*). interstitial macrophages (pink arrows). (*D*) $CD206^+CD68^+CD163^-$ macrophages in (*E*) snap-frozen or (*F*) FFPE IMC images were quantified using pixel quantification or cell segmentation. Bars indicate means ± SEM; each dot represents an individual sample. $^*P < 0.05$ and $^{**}P < 0.01$ by Mann-Whitney *U* test.

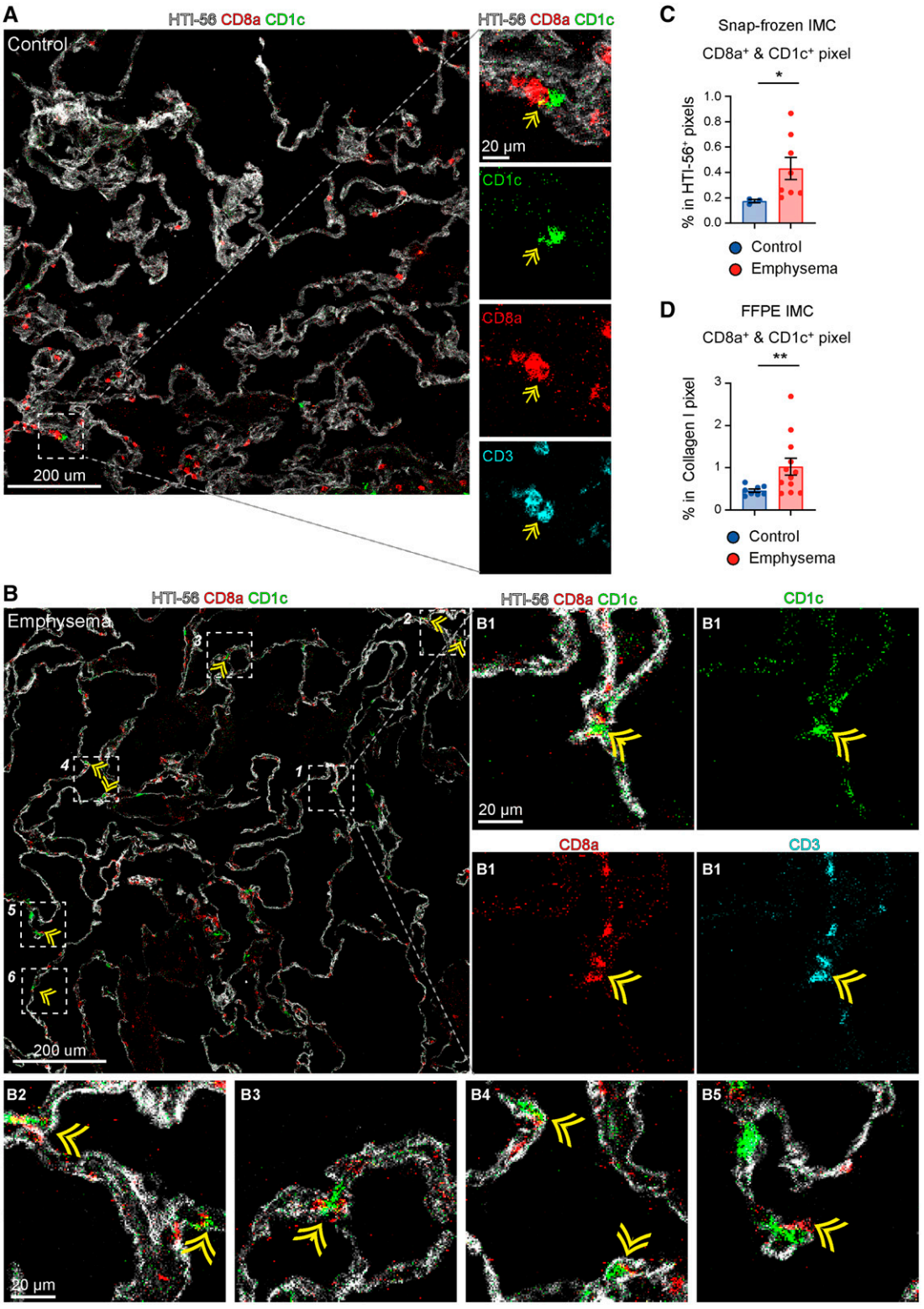

Figure 6. Spatial imaging analysis reveals altered cellular interactions in alveolar tissue from patients with emphysema. Imaging mass cytometry (IMC) was performed and several (immune, structural) markers were visualized: $CD1c^+$ dendritic cells (DCs; green), CD8a T cells (red), $HTI\text{-}56^+$ alveolar type I cells or collagen-I (white), $CD3^+$ T lymphocytes (light blue) in (*A*) control and (*B*) alveolar tissue from patients with emphysema. Colocalization of CD8 T cells and $CD1c^+$ DCs is indicated by double arrows. Cellular interactions between CD8 T cells and $CD1c^+$ DCs in (*C*) snap-frozen or (*D*) FFPE IMC images were quantified by pixel analysis using coexpression of both markers. Bars indicate means ± SEM; each dot represents an individual sample. $^*P < 0.05$ and $^{**}P < 0.01$ by Mann-Whitney *U* test. FFPE = formalin-fixed paraffin-embedded.

disease-associated differences between the COPD-emphysema and control groups.

Conclusions

Using CyTOF, we characterized the alterations of the immune cell signature in alveolar tissue from patients with emphysema versus control lung tissue. We also visualized the spatial location of emphysema-associated cell types, including $CD1c^+$ DCs and CD8 T cells *in situ* by IMC. These data thus contribute to a better understanding of pathogenesis of emphysema development and highlight the feasibility of interrogating the immune cell signature using CyTOF and IMC in human lung tissue. ■

Author disclosures are available with the text of this article at www.atsjournals.org.

Acknowledgment: The authors thank A. van Schadewijk (Department of Pulmonology, Leiden University Medical Center [LUMC], Leiden, the Netherlands); M. Schreurs (Department of Immunology, LUMC, Leiden, the Netherlands); the Flow Core Facility of the LUMC, Leiden, the Netherlands, coordinated by K. Schepers, T. Tak, and M. Hameetman; and the Flow Core Facility Operators for technical support for the (imaging) mass cytometry studies.

References

1. World Health Organization. The top 10 causes of death. 2020 [accessed 2022 Jul 25]. Available from: https://www.who.int/news-room/fact-sheets/detail/the-top-10-causes-of-death.
2. Celli BR, Wedzicha JA. Update on clinical aspects of chronic obstructive pulmonary disease. *N Engl J Med* 2019;381:1257–1266.
3. Willemse BW, ten Hacken NH, Rutgers B, Lesman-Leegte IG, Postma DS, Timens W. Effect of 1-year smoking cessation on airway inflammation in COPD and asymptomatic smokers. *Eur Respir J* 2005;26:835–845.
4. Buzza MS, Zamurs L, Sun J, Bird CH, Smith AI, Trapani JA, *et al.* Extracellular matrix remodeling by human granzyme B via cleavage of vitronectin, fibronectin, and laminin. *J Biol Chem* 2005;280:23549–23558.
5. Ravensberg AJ, Slats AM, van Wetering S, Janssen K, van Wijngaarden S, de Jeu R, *et al.* CD8(+) T cells characterize early smoking-related airway pathology in patients with asthma. *Respir Med* 2013;107:959–966.
6. Kim WD, Chi HS, Choe KH, Oh YM, Lee SD, Kim KR, *et al.* A possible role for CD8+ and non-CD8+ cell granzyme B in early small airway wall remodelling in centrilobular emphysema. *Respirology* 2013;18:688–696.
7. Shan M, Cheng HF, Song LZ, Roberts L, Green L, Hacken-Bitar J, *et al.* Lung myeloid dendritic cells coordinately induce TH1 and TH17 responses in human emphysema. *Sci Transl Med* 2009;1:4ra10.
8. Qiu SL, Kuang LJ, Tang QY, Duan MC, Bai J, He ZY, *et al.* Enhanced activation of circulating plasmacytoid dendritic cells in patients with chronic obstructive pulmonary disease and experimental smoking-induced emphysema. *Clin Immunol* 2018;195:107–118.
9. Liégeois M, Bai Q, Fievez L, Pirottin D, Legrand C, Guiot J, *et al.* Airway macrophages encompass transcriptionally and functionally distinct subsets altered by smoking. *Am J Respir Cell Mol Biol* 2022;67:241–252.
10. Belchamber KBR, Donnelly LE. Macrophage dysfunction in respiratory disease. *Results Probl Cell Differ* 2017;62:299–313.
11. Hodge S, Hodge G, Ahern J, Jersmann H, Holmes M, Reynolds PN. Smoking alters alveolar macrophage recognition and phagocytic ability: implications in chronic obstructive pulmonary disease. *Am J Respir Cell Mol Biol* 2007;37:748–755.
12. Lourenço JD, Ito JT, Martins MA, Tibério IFLC, Lopes FDTQDS. Th17/Treg imbalance in chronic obstructive pulmonary disease: clinical and experimental evidence. *Front Immunol* 2021;12:804919.
13. Isajevs S, Taivans I, Strazda G, Kopeika U, Bukovskis M, Gordjusina V, *et al.* Decreased FOXP3 expression in small airways of smokers with COPD. *Eur Respir J* 2009;33:61–67.
14. Bandura DR, Baranov VI, Ornatsky OI, Antonov A, Kinach R, Lou X, *et al.* Mass cytometry: technique for real time single cell multitarget immunoassay based on inductively coupled plasma time-of-flight mass spectrometry. *Anal Chem* 2009;81:6813–6822.
15. Guo N, Jia L, Out-Luiting C, Miranda NFCC, Willemze R, Koning F, *et al.* Mass cytometric analysis of early-stage mycosis fungoides. *Cells* 2022;11:1062.
16. Li N, van Unen V, Guo N, Abdelaal T, Somarakis A, Eggermont J, *et al.* Early-life compartmentalization of immune cells in human fetal tissues revealed by high-dimensional mass cytometry. *Front Immunol* 2019;10:1932.
17. de Vries NL, van Unen V, Ijsselsteijn ME, Abdelaal T, van der Breggen R, Farina Sarasqueta A, *et al.* High-dimensional cytometric analysis of colorectal cancer reveals novel mediators of antitumour immunity. *Gut* 2020;69:691–703.
18. Li N, van Unen V, Höllt T, Thompson A, van Bergen J, Pezzotti N, *et al.* Mass cytometry reveals innate lymphoid cell differentiation pathways in the human fetal intestine. *J Exp Med* 2018;215:1383–1396.
19. van Unen V, Li N, Molendijk I, Temurhan M, Höllt T, van der Meulen-de Jong AE, *et al.* Mass cytometry of the human mucosal immune system identifies tissue- and disease-associated immune subsets. *Immunity* 2016;44:1227–1239.
20. Chang Q, Ornatsky OI, Siddiqui I, Loboda A, Baranov VI, Hedley DW. Imaging mass cytometry. *Cytometry A* 2017;91:160–169.
21. Guo N, van Unen V, Ijsselsteijn ME, Ouboter LF, van der Meulen AE, Chuva de Sousa Lopes SM, *et al.* A 34-marker panel for imaging mass cytometric analysis of human snap-frozen tissue. *Front Immunol* 2020;11:1466.
22. Khedoe PPSJ, Li N, Jia L, Guo N, Hiemstra PS, Koning F, *et al.* High-dimensional mass cytometry analysis of immune cells in emphysematous lung tissue [abstract]. *Eur Respir J* 2020;56:4474.
23. van Unen V, Höllt T, Pezzotti N, Li N, Reinders MJT, Eisemann E, *et al.* Visual analysis of mass cytometry data by hierarchical stochastic neighbour embedding reveals rare cell types. *Nat Commun* 2017;8:1740.
24. Liechti T, Roederer M. OMIP-060: 30-Parameter flow cytometry panel to assess T cell effector functions and regulatory T cells. *Cytometry A* 2019;95:1129–1134.
25. Ijsselsteijn ME, van der Breggen R, Farina Sarasqueta A, Koning F, de Miranda NFCC. A 40-marker panel for high dimensional characterization of cancer immune microenvironments by imaging mass cytometry. *Front Immunol* 2019;10:2534.
26. Krop J, van der Meeren LE, van der Hoorn MP, Ijsselsteijn ME, Dijkstra KL, Kapsenberg H, *et al.* Identification of a unique intervillous cellular signature in chronic histiocytic intervillositis. *Placenta* 2023;139:34–42.
27. Krop J, van der Zwan A, Ijsselsteijn ME, Kapsenberg H, Luk SJ, Hendriks SH, *et al.* Imaging mass cytometry reveals the prominent role of myeloid cells at the maternal-fetal interface. *iScience* 2022;25:104648.
28. Qiu W, Kang N, Wu Y, Cai Y, Xiao L, Ge H, *et al.* Mucosal associated invariant T cells were activated and polarized toward Th17 in chronic obstructive pulmonary disease. *Front Immunol* 2021;12:640455.
29. Xu G, Qi F, Li H, Yang Q, Wang H, Wang X, *et al.* The differential immune responses to COVID-19 in peripheral and lung revealed by single-cell RNA sequencing. *Cell Discov* 2020;6:73.
30. Richmond BW, Mansouri S, Serezani A, Novitskiy S, Blackburn JB, Du RH, *et al.* Monocyte-derived dendritic cells link localized secretory IgA deficiency to adaptive immune activation in COPD. *Mucosal Immunol* 2021;14:431–442.
31. Paats MS, Bergen IM, Hoogsteden HC, van der Eerden MM, Hendriks RW. Systemic CD4+ and CD8+ T-cell cytokine profiles correlate with GOLD stage in stable COPD. *Eur Respir J* 2012;40:330–337.
32. Kalathil SG, Lugade AA, Pradhan V, Miller A, Parameswaran GI, Sethi S, *et al.* T-regulatory cells and programmed death 1+ T cells contribute to effector T-cell dysfunction in patients with chronic obstructive pulmonary disease. *Am J Respir Crit Care Med* 2014;190:40–50.

33. Fergusson JR, Fleming VM, Klenerman P. CD161-expressing human T cells. *Front Immunol* 2011;2:36.
34. Di Stefano A, Caramori G, Gnemmi I, Contoli M, Vicari C, Capelli A, *et al.* T helper type 17-related cytokine expression is increased in the bronchial mucosa of stable chronic obstructive pulmonary disease patients. *Clin Exp Immunol* 2009;157:316–324.
35. Koch A, Gaczkowski M, Sturton G, Staib P, Schinköthe T, Klein E, *et al.* Modification of surface antigens in blood CD8+ T-lymphocytes in COPD: effects of smoking. *Eur Respir J* 2007;29:42–50.
36. Li L, Liu Y, Chiu C, Jin Y, Zhou W, Peng M, *et al.* A regulatory role of chemokine receptor CXCR3 in the pathogenesis of chronic obstructive pulmonary disease and emphysema. *Inflammation* 2021;44:985–998.
37. Xie JH, Nomura N, Lu M, Chen SL, Koch GE, Weng Y, *et al.* Antibody-mediated blockade of the CXCR3 chemokine receptor results in diminished recruitment of T helper 1 cells into sites of inflammation. *J Leukoc Biol* 2003;73:771–780.
38. Freeman CM, Han MK, Martinez FJ, Murray S, Liu LX, Chensue SW, *et al.* Cytotoxic potential of lung CD8(+) T cells increases with chronic obstructive pulmonary disease severity and with in vitro stimulation by IL-18 or IL-15. *J Immunol* 2010;184:6504–6513.
39. Kim WD, Chi HS, Choe KH, Kim WS, Hogg JC, Sin DD. The role of granzyme B containing cells in the progression of chronic obstructive pulmonary disease. *Tuberc Respir Dis (Seoul)* 2020;83:S25–S33.
40. Doering TA, Crawford A, Angelosanto JM, Paley MA, Ziegler CG, Wherry EJ. Network analysis reveals centrally connected genes and pathways involved in CD8+ T cell exhaustion versus memory. *Immunity* 2012;37:1130–1144.
41. Wang C, Hyams B, Allen NC, Cautivo K, Monahan K, Zhou M, *et al.* Dysregulated lung stroma drives emphysema exacerbation by potentiating resident lymphocytes to suppress an epithelial stem cell reservoir. *Immunity* 2023;56:576–591.e10.
42. Rustam S, Hu Y, Mahjour SB, Rendeiro AF, Ravichandran H, Urso A, *et al.* A unique cellular organization of human distal airways and its disarray in chronic obstructive pulmonary disease. *Am J Respir Crit Care Med* 2023;207:1171–1182.
43. Booth S, Hsieh A, Mostaco-Guidolin L, Koo HK, Wu K, Aminazadeh F, *et al.* A single-cell atlas of small airway disease in chronic obstructive pulmonary disease: a cross-sectional study. *Am J Respir Crit Care Med* 2023;208:472–486.
44. Villaseñor-Altamirano AB, Jain D, Jeong Y, Menon JA, Kamiya M, Haider H, *et al.*; MassGeneralBrigham–Bayer Pulmonary Drug Discovery Laboratory. Activation of CD8+ T cells in chronic obstructive pulmonary disease lung. *Am J Respir Crit Care Med* 2023;208:1177–1195.
45. Rojas-Quintero J, Ochsner SA, New F, Divakar P, Yang CX, Wu TD, *et al.* Spatial transcriptomics resolve an emphysema-specific lymphoid follicle B cell signature in COPD. *Am J Respir Crit Care Med* 2024;209: 48–58.
46. Sullivan JL, Bagevalu B, Glass C, Sholl L, Kraft M, Martinez FD, *et al.* B cell-adaptive immune profile in emphysema-predominant chronic obstructive pulmonary disease. *Am J Respir Crit Care Med* 2019;200: 1434–1439.
47. Polverino F, Seys LJ, Bracke KR, Owen CA. B cells in chronic obstructive pulmonary disease: moving to center stage. *Am J Physiol Lung Cell Mol Physiol* 2016;311:L687–L695.
48. Kelsen SG, Aksoy MO, Georgy M, Hershman R, Ji R, Li X, *et al.* Lymphoid follicle cells in chronic obstructive pulmonary disease overexpress the chemokine receptor CXCR3. *Am J Respir Crit Care Med* 2009;179:799–805.
49. Hogg JC, Chu F, Utokaparch S, Woods R, Elliott WM, Buzatu L, *et al.* The nature of small-airway obstruction in chronic obstructive pulmonary disease. *N Engl J Med* 2004;350:2645–2653.
50. van der Strate BW, Postma DS, Brandsma CA, Melgert BN, Luinge MA, Geerlings M, *et al.* Cigarette smoke-induced emphysema: a role for the B cell? *Am J Respir Crit Care Med* 2006;173:751–758.
51. Gosman MM, Willemse BW, Jansen DF, Lapperre TS, van Schadewijk A, Hiemstra PS, *et al.*; Groningen and Leiden Universities Corticosteroids in Obstructive Lung Disease Study Group. Increased number of B-cells in bronchial biopsies in COPD. *Eur Respir J* 2006;27:60–64.
52. Demedts IK, Bracke KR, Van Pottelberge G, Testelmans D, Verleden GM, Vermassen FE, *et al.* Accumulation of dendritic cells and increased CCL20 levels in the airways of patients with chronic obstructive pulmonary disease. *Am J Respir Crit Care Med* 2007;175: 998–1005.
53. Van Pottelberge GR, Bracke KR, Demedts IK, De Rijck K, Reinartz SM, van Drunen CM, *et al.* Selective accumulation of langerhans-type dendritic cells in small airways of patients with COPD. *Respir Res* 2010;11:35.
54. Thaiss CA, Semmling V, Franken L, Wagner H, Kurts C. Chemokines: a new dendritic cell signal for T cell activation. *Front Immunol* 2011; 2:31.
55. Kuang LJ, Deng TT, Wang Q, Qiu SL, Liang Y, He ZY, *et al.* Dendritic cells induce Tc1 cell differentiation via the CD40/CD40L pathway in mice after exposure to cigarette smoke. *Am J Physiol Lung Cell Mol Physiol* 2016;311:L581–L589.
56. Sauler M, McDonough JE, Adams TS, Kothapalli N, Barnthaler T, Werder RB, *et al.* Characterization of the COPD alveolar niche using single-cell RNA sequencing. *Nat Commun* 2022;13:494.
57. Blomme EE, Provoost S, De Smet EG, De Grove KC, Van Eeckhoutte HP, De Volder J, *et al.* Quantification and role of innate lymphoid cell subsets in chronic obstructive pulmonary disease. *Clin Transl Immunology* 2021;10:e1287.
58. Mills CD, Kincaid K, Alt JM, Heilman MJ, Hill AM. M-1/M-2 macrophages and the Th1/Th2 paradigm. *J Immunol* 2000;164:6166–6173.